Design and Development of Low-Cost Optical-Fiber Sensors for Temperature Metrology: Process Monitoring of an Epoxy Resin System

B. Degamber, J. Tetlow, G. F. Fernando

Engineering Systems Department, Cranfield University, Royal Military College of Science, Shrivenham, Swindon, SN6 8LA, United Kingdom

Received 10 September 2003; accepted 31 March 2004
DOI 10.1002/app.20745
Published online in Wiley InterScience (www.interscience.wiley.com).

ABSTRACT: This article reports the design and deployment of two optical-fiber temperature sensors based on the fiber Fabry–Perot etalon. The first involved the use of an extrinsic fiber Fabry–Perot sensor, but in this instance, the coefficient of thermal expansion of the reflector and/or capillary was chosen to offer a mismatch. Hence, the cavity length could increase or decrease according to the coefficient of thermal expansion of the fiber and/or capillary. For comparison, single-mode and multimode optical-fiber Bragg gratings were also used as temperature sensors. The Fabry–Perot sensors operated from −50 to 410°C. The accuracy of the measurements was up to ±0.5°C with a low-cost charged-coupling-device spectrometer. The sensors also worked effectively in a microwave oven and in a composite panel in an autoclave. © 2004 Wiley Periodicals, Inc. J Appl Polym Sci 94: 83–95, 2004

Key words: curing of polymers; sensors; thermal properties

INTRODUCTION

Sensor systems based on optical fibers are increasingly being used for the process monitoring and nondestructive structural health assessment of engineering materials and structures.[1] There are a number of reasons for this interest in the use of optical-fiber sensors: (1) their immunity from electromagnetic radiation; (2) their ease of integration into and onto materials and structures; (3) their capacity for remote and real-time interrogation; (4) the option of multiplexing a number of sensors on a single fiber; and (5) their capacity to enable multiple-measure monitoring.

With a specific reference to the optical-fiber-based condition assessment of materials and structures, a number of sensor systems have been demonstrated and proved to be effective tools.[2] However, the costs associated with optical-fiber sensors can be high, and their deployment has been restricted to specialist applications for which conventional electrical-based techniques cannot be used.

Correspondence to: G. F. Fernando.
Contract grant sponsor: Engineering and Physical Sciences Research Council.
Contract grant sponsor: Engineering Systems Department at Cranfield University.
Contract grant sponsor: Engineering and Aerospace Club.

Table I presents a cost comparison of conventional electrical-based sensors and their optical-fiber equivalents for monitoring the temperature.[3] Details for the suppliers are not included, and the cost was calculated on the basis of single-, two-, and eight-channel systems. According to the data presented in Table I, fiber-optic sensors and sensor interrogating systems are more expensive than their metallic counterparts. Although optical-fiber sensors offer numerous advantages over electrical-based sensors, their overall cost has to be reduced significantly if they are to be adopted and used routinely in material processing industries. Therefore, there is significant merit in developing relatively low-cost and generic optical-fiber sensors that can be used in a range of material processing and structural health monitoring applications.

One area in which the use of thermocouples is not a viable option is an electromagnetic environment, in which the presence of metal and metallic pointed ends can greatly distort fields. In such cases, it is preferable to use nonmetallic sensors, especially those based on optical fibers. This is because these sensors are immune to electromagnetic interference and cause minimum perturbation to fields because of their small size and low dielectric properties.[4] A number of articles have reported the use of fiber-optic sensors for temperature metrology during microwave processing, and some of these are listed in Table II. The types of applicators, the resin systems, and the cure monitoring techniques are also de-

TABLE I
Summary of Relative Costs Associated with the Interrogation Units for Optical-Fiber- and Electrical-Based Sensor Systems

Temperature sensor	Single-channel interrogation unit (£)	Eight-channel interrogation unit (£)	Single sensor (£)	Operating principle for the interrogation unit and accuracy/resolution
Electrical	500 (including a PC)	1200 (including a PC)	5	Data logged to a PC with a data acquisition card; ± 1°C
Optical				
FP	3,500	7,500	250–350	Data logged to a PC through RS 232; ± 1°C
FTM	7,000	10,200	450–500	Data logged to a PC through RS 232; ± 1°C

The data presented under each category are averages of two or more suppliers. FP = Fabry–Perot sensors; FTM = fluorescence-temperature monitoring.

scribed. Table II shows a popular fiber-optic temperature sensor available form Luxtron. However, other commercial sensors are available, and some of these are mentioned in Table III.[10]

Although these sensors are extremely reliable for temperature metrology in a microwave environment, the cost of these sensors and their interrogation units hampers their use as disposable devices. Hence, it is necessary to investigate low-cost options for temperature monitoring during microwave processing.

This article presents and compares the suitability of (1) two Fabry–Perot (FP)-based fiber-optic sensors and (b) single-mode and multimode fiber Bragg grating sensors as tools for remote and online temperature metrology. The performance of the most viable sensor of the four was further evaluated during the microwave-based processing of an epoxy resin system. The sensor was finally used in an autoclave by being embedded in a laminated prepreg between the fourth ply and fifth ply of an eight-ply E-glass fiber composite laminate.

BACKGROUND

Sensor design

Extrinsic-fiber FP temperature sensor

A schematic illustration of the conventional extrinsic Fabry–Perot interferometer (EFPI) sensor design is presented in Figure 1. It essentially consists of two cleaved optical fibers that are secured in a precision-bore fused silica capillary tube with a specified air cavity between the fiber ends. The fibers are secured inside the capillary by a fusion joint with a conven-

TABLE II
Summary of the Research Carried Out on Microwave Curing and the Cure Monitoring Techniques Used

Author	Applicator	Resin system	Temperature probe	Cure monitoring technique
Hedreul et al.[5]	Waveguide	DER 332 with DDS	Luxtron model 755 fluoroptic (±1°C)	Size exclusion chromatography up to gelation; DSC used for the degree of conversion
Rogers et al.[6]	Single-mode rectangular and cylindrical cavities	MY721/27% DDS	Luxtron (model number not provided) temperature probe	FT-NIR transmission spectroscopy with two optical fibers in a PTFE microcapillary
Mijovic et al.[7]	Waveguide	DGEBA/4,4′-methylenedianiline	Luxtron model 750 fluoroptic thermometer	High-performance liquid chromatography and FTIR spectroscopy
Fu and Hawley[8]	Single-mode cylindrical cavity	DGEBA/DDS	Luxtron model 755 fluoroptic (±1°C)	FTIR spectroscopy
Wei et al.[9]	Single-mode cylindrical tuneable cavity	DGEBA/DDS	Luxtron 785 fluorescence probe	FTIR spectroscopy on samples cured to different extents and quenched

DER 332 = Dow Epoxy Resin; DDS = Diaminodiphenyl sulfone; PTFE = Polytetrafluoroethylene; DGEBA = Diglycidyl ether of bisphenol-A.

TABLE III
Commercially Available Fiber-Optic Systems

System	Sensor construction	No. of channels and measurements made
Luxtron	A phosphor attached to the end of a quartz fiber	4, 8, or 12 channels Temperature, electric-field probes
Metricor	A cavity resonator consisting of a layer of material whose refractive index varies with temperature	4 channels Temperature, pressure, refractive-index probes
Ipitek	A temperature-sensitive semiconductor platelet attached to the end of a quartz probe	1 channel, modular (1–14) to follow Temperature probes
Takaoka	A GaAs crystal assembled to a quartz fiber, inserted in an air-filled glass tube	Modular (1–24 channels) Temperature probes
Fiso[a]	FP cavity between two reflectors in a capillary	4, 16 channels Temperature, pressure, strain probes

[a] Added to the table quoted in the article from which the table was taken.

tional fusion splicer. The gauge length is taken as the distance between the two fusion joints.

With reference to Figure 2, the mode of operation of the EFPI sensor can be described as follows. A superluminescence diode (SLD) light source is used to illuminate the end of one fiber. Approximately 4% of the light being transmitted down the fiber is reflected back at the first cleaved fiber/air interface. A similar proportion of the remaining transmitted light is reflected back from the second cleaved air/fiber interface into the light guide. The superposition of the two reflected beams causes interference to occur in the light guide, and an interference pattern is formed on the charged-coupling-device (CCD) spectrometer. The resultant interference pattern that is formed varies with the distance between the two cleaved end faces. The absolute cavity length (d; i.e., the distance between the fiber end faces) of the EFPI sensor can be measured from the wavelength separation by the scanning of one complete interference fringe and is determined as follows where λ_1 and λ_2 are the wavelengths of the two valleys on each side of an interference fringe:[11]

$$d = \frac{\lambda_2 \lambda_1}{2000(\lambda_1 - \lambda_2)}\ \mu\text{m} \tag{1}$$

The sensor design illustrated in Figure 1 is relatively insensitive to temperature because the thermal expansions of the capillary and optical fibers are similar. The relative axial expansion of the capillary is compensated by that of the cleaved fibers in the opposite direction. Furthermore, the sensitivity of the air cavity to temperature is negligible over the range of interest, from subambient temperatures to 400°C. This EFPI sensor is, therefore, mainly used as a strain sensor because it does not suffer from cross sensitivity with temperature (see Fig. 3). The inset in Figure 3 shows a magnified picture of the variation of the cavity length of the sensor with the temperature. The change is very small, less than 0.3 μm. This change can be attributed to thermal drift in the instrumentation.

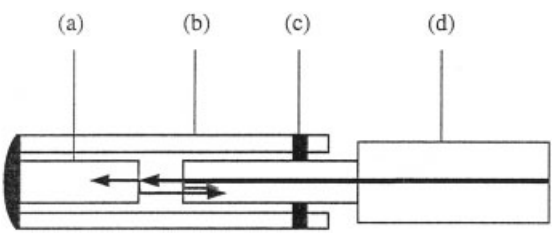

Figure 1 Schematic illustration of an EFPI sensor: (a) the reflector fiber, (b) the silica capillary, (c) the fusion point, and (d) the lead-in fiber.

However, the EFPI sensor can be modified for temperature measurement through the mismatching of the thermal expansion of the reflector fiber or capillary materials involved [Fig. 1(a,b)].

In the first design, the silica capillary is replaced with one made of borosilicate. Because borosilicate has a higher coefficient of thermal expansion ($\alpha = 3.5 \times 10^{-6}$°C^{-1}), the capillary will tend to force the silica fibers away from one another as the temperature is increased. This in turn causes an increase in the air cavity between the end faces of the fibers.

The increase in the cavity length due to a thermal expansion mismatch between borosilicate and silica is determined as follows:

$$\Delta d = [(\alpha_{\text{bo}} - \alpha_{\text{si}})L + \alpha_{\text{bo}}\, d]\Delta T \tag{2}$$

where α_{bo} and α_{si} are the coefficients of thermal expansion of borosilicate and silica, respectively. ΔT is the temperature change, d is the cavity length between the fiber ends, and L is the gauge length (the length between the fusion points) of the sensor.

In the second design, the reflector fiber [Fig. 1(a)] is replaced with a soda silicate glass rod with a cleaved end face. When this sensor is subjected to a temperature increase, the greater thermal expansion of soda silicate glass ($\alpha = 9.5 \times 10^{-6}$°C^{-1}), compared with that

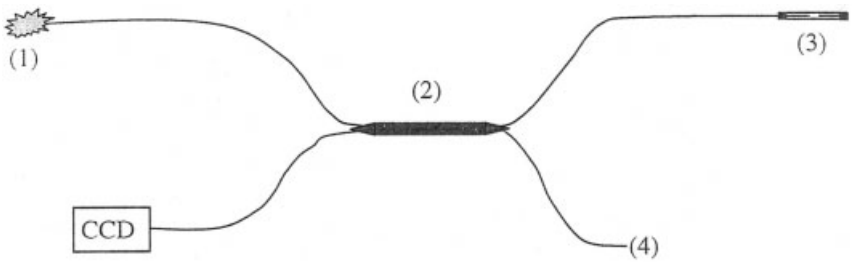

Figure 2 Schematic of the arrangement used to record the spectra from the temperature sensor: (1) the light source, (2) the 2 × 2 coupler, (3) the sensor, and (4) the broken end of the fiber used to prevent any back-reflection.

for silica (0.55×10^{-6}°C^{-1}), causes the cavity length to decrease. The variation in the cavity length with the temperature is determined as follows:

$$\Delta d = [(\alpha_{so} - \alpha_{si})l]\Delta T \tag{3}$$

where α_{so} and α_{si} are the thermal expansion coefficients of the soda silicate glass rod and the capillary, respectively, and l is the length of the free-moving soda silicate glass rod.

Single and multimode fiber bragg gratings

Single-mode Bragg grating sensor. Bragg gratings are generally written in a single-mode fiber[12] with a phase mask and a coherent laser source or through the impingement of two coherent UV lasers onto a declad section of the fiber. This interaction of the interference pattern on the optical-fiber core results in a periodic modulation of the refractive index of the core. Upon the illumination of this fiber with a broadband light source, in agreement with the Bragg criterion, only one wavelength, the Bragg wavelength (λ_B), can interfere constructively:[13]

$$\lambda_B = 2n\Lambda \tag{4}$$

where n is the effective core refractive index and Λ is the period of the modulation of the refractive index. Therefore, any factor that causes the periodicity of the grating to be altered can be monitored accurately through the inspection of the reflected or transmitted spectrum through the Bragg grating.[14]

For ΔT, the corresponding wavelength shift ($\Delta\lambda_{BT}$) is determined as follows:

$$\Delta\lambda_{BT} = \lambda_B(\alpha + \zeta)\Delta T \tag{5}$$

where $\alpha = (1/\Lambda)(\partial\Lambda/\partial T)$ is the thermal expansion coefficient for the fiber (ca. 0.55×10^{-6}°C^{-1} for silica). The quantity $\zeta = (1/n)(\partial\Lambda/\partial T)$ is called the thermooptical coefficient and represents the change in the refractive index (optical density) with temperature. For germanium-doped silica core fiber, ζ is 8.6

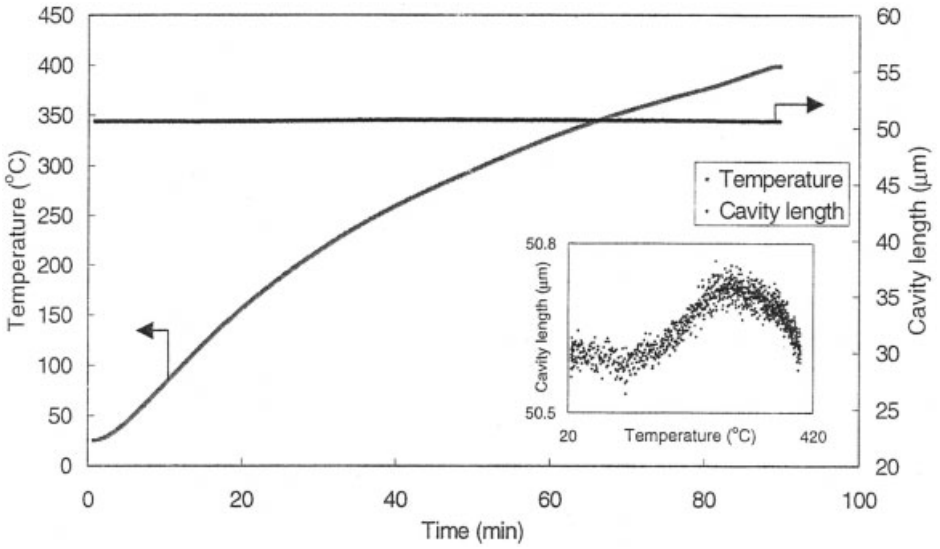

Figure 3 Variation of the cavity length of a conventional EFPI sensor when subjected to a temperature ramp. The inset shows that the change in the cavity length is very small over the temperature range.

$\times 10^{-6}$°C^{-1}. For a fiber Bragg grating operating at 850 nm, fiber Bragg grating sensitivities ranging from 5.5 to 6.8 pm °C^{-1} have been reported.[7,15]

Fiber Bragg gratings are also sensitive to axial, lateral, and radial strains. Therefore, for temperature metrology, the grating has to be isolated from the strain, and this is generally achieved by it being housed in a capillary tube.[16]

Multimode Bragg grating sensors. Bragg gratings have been inscribed in multimode fibers, and unlike their single-mode counterparts, they exhibit multiple reflection peaks or multiple transmission dips in the reflection or transmission spectra, respectively.[17] The thermally induced shift of a multimode fiber Bragg grating can be described as follows:[18]

$$\frac{d\lambda}{dT} = \frac{\lambda^2}{2n_1\Lambda^2}\frac{d\Lambda}{dT} + \left[\frac{\lambda^2}{2n_1^2\Lambda} - \frac{\lambda^2(N+1)(3n_2-2n_1)}{2\pi a n_1^2\sqrt{2n_1(n_1-n_2)}}\right]\frac{dn_1}{dT} + \frac{\lambda^2(N+1)}{2\pi a n_1\sqrt{2n_1(n_1-n_2)}}\frac{dn_2}{dT} \quad (6)$$

where n_1 and n_2 are the refractive indices of the core and cladding, respectively; Λ is the period of the grating; N is the number of the principal mode; and a is the radius of the core.

The temperature sensitivity of multimode fiber Bragg gratings operating at 1550 and 750 nm[11,19] has been reported to be 11.5 and 3 pm °C^{-1}, respectively.

The multimode fiber Bragg gratings were fabricated through the illumination of a 50/125 graded index multimode fiber with a KrF excimer laser with the phase mask method. The fiber was first sensitized by conditioning at 100 atm for 2 weeks in a hydrogen environment. The laser beam was directed onto the surface of a UV-enhanced reflecting mirror and focused to approximately 5 mm $\times$ 100 μm with a cylindrical UV lens. The fiber and the phase mask were placed on a translation stage, which allowed movement perpendicular to the incident light on the phase mask. The scanning rate of the stage could be altered to produce a desired length of the Bragg grating along the fiber axis.

Processing of the thermosets and composites

Microwave processing

For several decades, the microwave processing of thermosets has been used as an alternative to conventional thermal processes. Although conventional heating remains the preferred processing method, the use of microwave energy to heat composite matrices can be very useful. Microwave heating occurs through the conversion of electromagnetic energy into heat when the energy interacts with the polar molecules present in the materials. The advantage of microwave heating is that the whole sample is penetrated simultaneously by the radiation, and this minimizes the long delay that occurs because of convection and conduction in conventional processing. When a material is heated by microwave radiation, the molecules in the material are excited and polarized by the alternating electric field. The inability of the excited molecules to follow the rapid field reversal results in the generation of heat through the material. This gives rise to substantially reduced cycle times, leading to less energy being used and, therefore, potentially lower costs.[20]

One problem associated with microwave curing is the monitoring of the temperature during the curing process. The use of a thermocouple for temperature monitoring inside a microwave oven or cavity is not advisable as the presence of metallic tips can disturb the microwave field, resulting in hot or cold spots. Therefore, optical-fiber temperature sensors are used as alternatives to metallic probes. However, commercial optical-fiber sensors and their interrogation units can be very expensive. This means that these sensors cannot be used as disposable sensors.

Autoclave processing

Conventionally, epoxy–amine systems are processed by the application of heat or, in some cases, pressure in a controlled oven or autoclave. Autoclave molding is globally accepted as a process for manufacturing high-quality composites. The starting material in an autoclave is normally a prepreg, which is a preimpregnated sheet of a combination of the reinforcing fibers and the resin matrix. In an autoclave curing process, the prepreg is laid in the required orientation and vacuum-bagged. The entire assembly is placed inside an autoclave, in which a combination of heat, pressure, and vacuum consolidates and cures the laminate. During the cure, the resin mixture is transformed from a liquid to a gelled solid and finally vitrifies through an irreversible process. The ultimate properties of the cured material depend largely on the chemical formulation of the resin system and the processing conditions used, including the operating temperature.

EXPERIMENTAL

Temperature calibration

A schematic illustration of the experimental setup for the temperature calibration and sensor interrogation is presented in Figure 2. The sensors were tested in a tubular furnace equipped with a Eurotherm temperature controller (Eurotherm, Ltd., Faraday Close, West Sussex, United Kingdom) with an accuracy of 1.0°C.

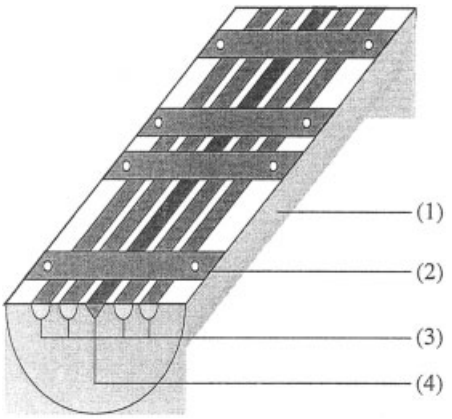

Figure 4 Schematic of the jig for the housing sensor and thermocouples during testing inside the tubular furnace: (1) the semicylindrical metal rod, (2) the metal strip screwed on the rod to fix the sensor and thermocouples in position, (3) the slots for the thermocouples, and (4) the slot for the optical finer sensor.

The sensor was calibrated against a K-type thermocouple. A jig was constructed to accommodate and secure the sensor and three thermocouples in close proximity inside the furnace (see Fig. 4). The jig was housed in a cylindrical glass tube to reduce heat loss to the surroundings.

Sensor interrogation

FP-based sensors

Interference spectra from the modified EFPI sensors were recorded with an Ocean Optics S2000 CCD spectrometer (Ocean Optics BV, RK Duiven, The Netherlands), which had a resolution of 0.14 nm and was powered by an SLD light source with a center wavelength of 850 nm. The two modified EFPI sensors were tested from the ambient temperature to 300 and 400°C, respectively. The sensor constructed with the soda silicate reflector was further tested for operation in the subambient temperature range, from −50°C to room temperature, in a liquid-nitrogen-cooled environmental chamber. This sensor was also subjected to a microwave field in a custom-modified oven. Because a thermocouple could not be used in the microwave oven, a commercially available temperature sensor (FOT-L, Fiso Technology, Ltd.) was used to calibrate the in-house sensor. Finally, the in-house sensor was inserted between the fourth ply and fifth ply of an eight-ply E-glass/composite laminate in an autoclave to record the temperature during the cure.

Fiber-bragg-grating-based sensors

The single-mode Bragg grating sensors were tested with the same setup used for the FP-based sensors. However, in the case of the grating, the position of the peak was recorded as a function of the temperature. The sensor was heated in a series of ramp holds from the ambient temperature to 160°C in the tubular furnace.

Because the operating range of the S2000 CCD spectrometer was between 780 and 900 nm, it could not be used to interrogate the multimode Bragg grating. The latter was operated around 1540 nm, and so a Nicolet Magna IR-750 Fourier transform infrared (FTIR) spectrometer was used to interrogate the sensor. The ends of the fiber grating were cleaved with a standard cleaver and connected to the near-infrared ports of the FTIR spectrometer with bullet subminiature A-type connectors. The experiment was conducted as a series of ramp holds from the ambient temperatures to 140°C.

Temperature monitoring during the processing of the thermosets and composites

Microwave curing

The temperature of an epoxy resin (LY 3505/XB 3403, Vantico UK, Ltd.) cured at 400 W in a custom-modified microwave oven (Sanyo EM-P1010, purchased from Sanyo Electric Manufacturing, Ltd., Durham, United Kingdom and modified by Gamma Consultants, Ltd., Kent, United Kingdom)[21] was recorded with both a commercial sensor and an in-house modified FP sensor. The resin was cured in a glass cell (22 mm in diameter and 3 mm thick) with a slit on the side of the cell for resin insertion. The in-house FP sensor (with the soda silicate reflector) was housed in a thin-wall quartz capillary and inserted directly in the resin (see Fig. 5). The commercial sensor (Fiso Technology) was glued onto the side of the glass cell in contact with the glass sample holder to obtain the temperature in close proximity to the curing resin.

Autoclave processing

Finally, the modified sensor was used to monitor the temperature inside a composite laminate cured in an

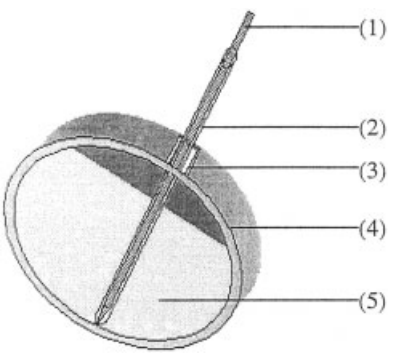

Figure 5 Arrangement for the containment of the LY3505/XB 3403 resin system during microwave processing: (1) the temperature probe, (2) the thin-wall glass tube, (3) the slit for resin and probe insertion, (4) the glass cell, and (5) the resin.

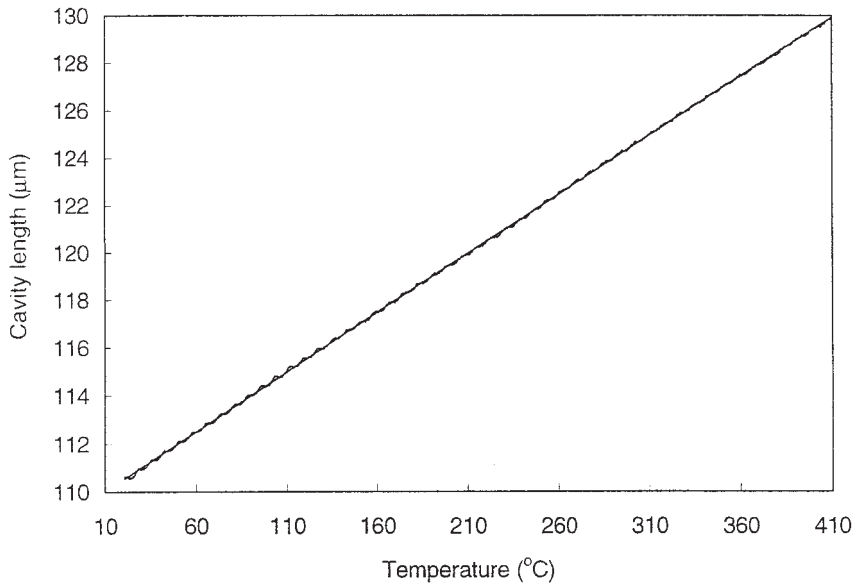

Figure 6 Effect of the temperature on a modified EFPI sensor constructed with a borosilicate capillary.

autoclave (Aeroform, Ltd., Hampshire, United Kingdom). The maximum operating temperature and pressure were 220°C and 220 psi, respectively. The composite was made of eight plies of an E-glass prepreg that were laminated with conventional techniques. The fiber sensor and a thermocouple were fixed between the fourth ply and fifth ply of the composite. The composite panel was first heated from 30 to 120°C in 30 min. The temperature was maintained at 120°C for 1 h before the autoclave was allowed to cool to 50°C. The autoclave pressure was set to 90 psi.

RESULTS AND DISCUSSION

Temperature response of the sensors

Sensor with a borosilicate capillary

The performance of the EFPI sensor constructed with a borosilicate capillary is presented in Figure 6. The sensor was made with a gauge length of 18 mm and a cavity length of 110 μm. The cavity length obtained from the experiment agrees with the value calculated with eq. (2). The response of the sensor

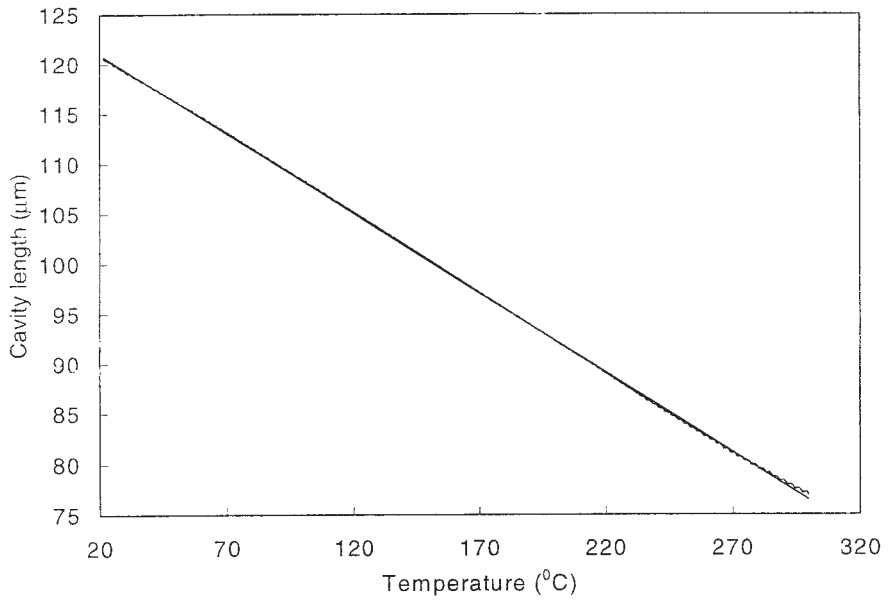

Figure 7 Response of an EFPI sensor with a soda silicate glass rod as a reflector.

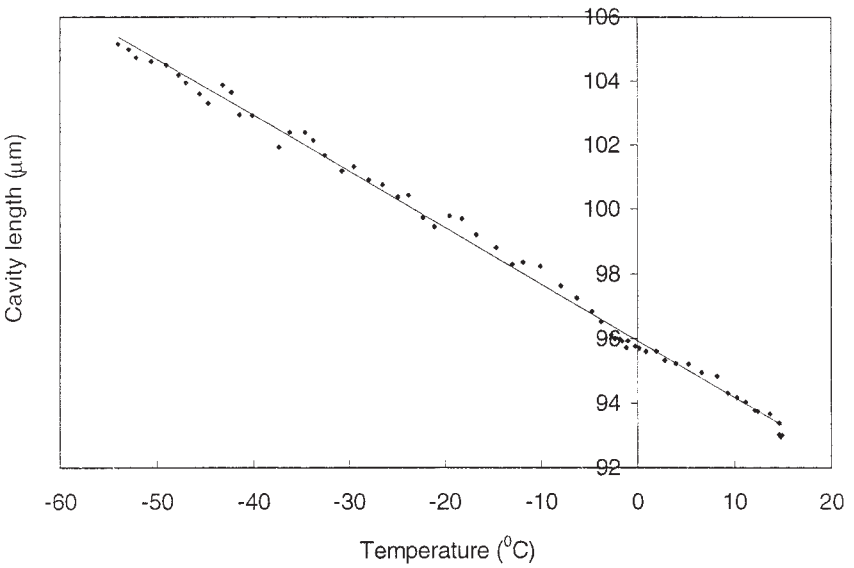

Figure 8 Response of a soda silicate sensor to subambient conditions.

was linear up to 410°C, and no hysteresis was observed. The sensor could not be tested at higher temperatures as the borosilicate glass started to soften. Above this temperature, the relationship between the cavity length and temperature was nonlinear. The accuracy of the sensor was ±1°C and was limited by the resolution of the CCD spectrometer, which was 0.14 nm.

The drawback of the sensor is that its sensitivity is relatively low, and so it cannot be used to measure small values of ΔT. In addition to the resolution of the CCD spectrometer used in this study, the difference in the thermal expansivities between borosilicate and silica was small. For this reason, an attempt was made to use soda silicate ($\alpha = 9.5 \times 10^{-6}$°C^{-1}) glass instead of borosilicate as the capillary. However, soda silicate melts at a lower temperature than silica, and the difference in the thermal expansion caused the fusion point between the optical fiber and the capillary to fracture. Furthermore, this sensor was too fragile to be handled and tested. Hence, the soda silicate glass EFPI reflector design was developed.

Sensor with a soda silicate reflector

The response of the soda silicate reflector EFPI sensor design, from the ambient temperature to 300°C, is

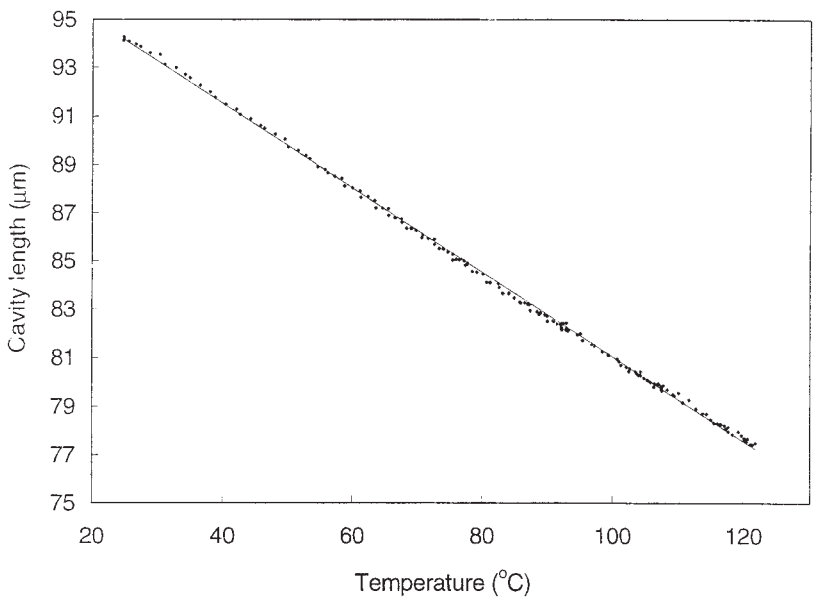

Figure 9 Response of a soda silicate EFPI sensor to temperature increments in a microwave oven.

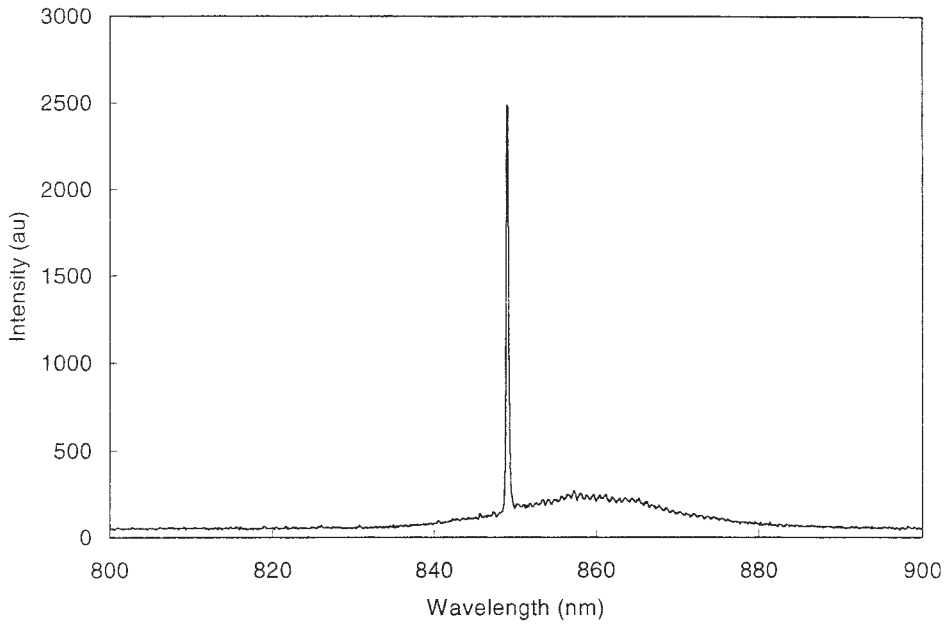

Figure 10 Typical CCD spectrum of a single-mode Bragg grating sensor.

presented in Figure 7. The line of best fit is plotted along the same axes for reference. As expected, the response was linear over that range with the coefficient of determination ($R^2 = 1$). This deviation observed after 280°C might be attributed to the low softening point of soda silicate glass. From the ambient temperature to 300°C, an excellent correlation was obtained between the observed and calculated values with eq. (3). The repeatability of this sensor design in terms of its performance was excellent. The accuracy of the sensor was estimated to be ±0.5°C. The sensitivity of the sensor was 162 nm °C^{-1}. This depended on the length of the soda silicate glass rod used.

Soda silicate sensor at subambient temperatures. As mentioned earlier, the modified EFPI sensor was further tested at subambient temperatures with a liquid-nitro-

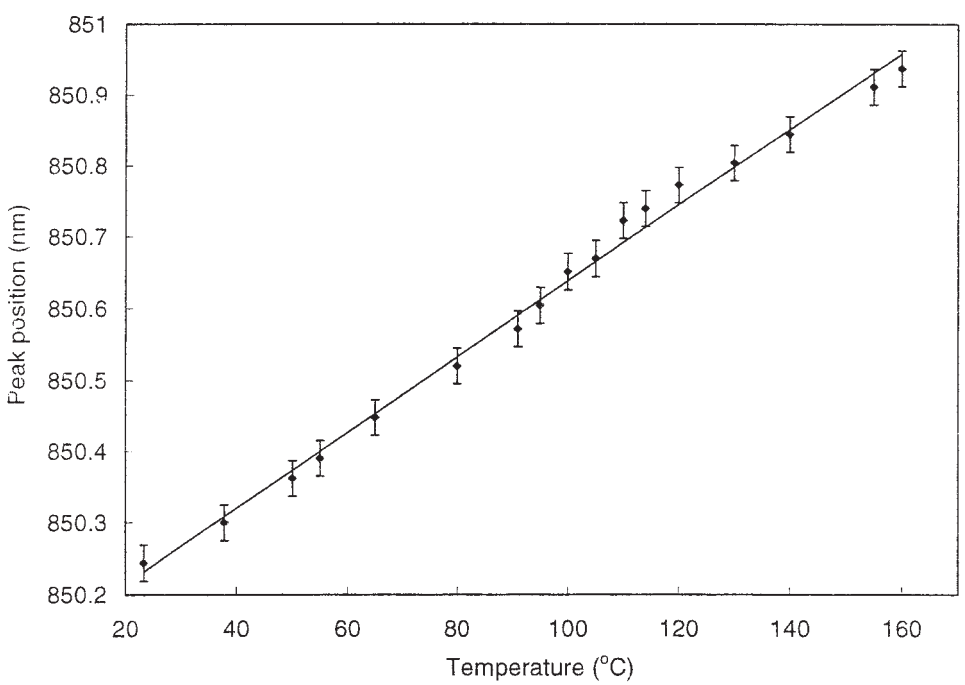

Figure 11 Response of a single-mode Bragg grating sensor to the temperature.

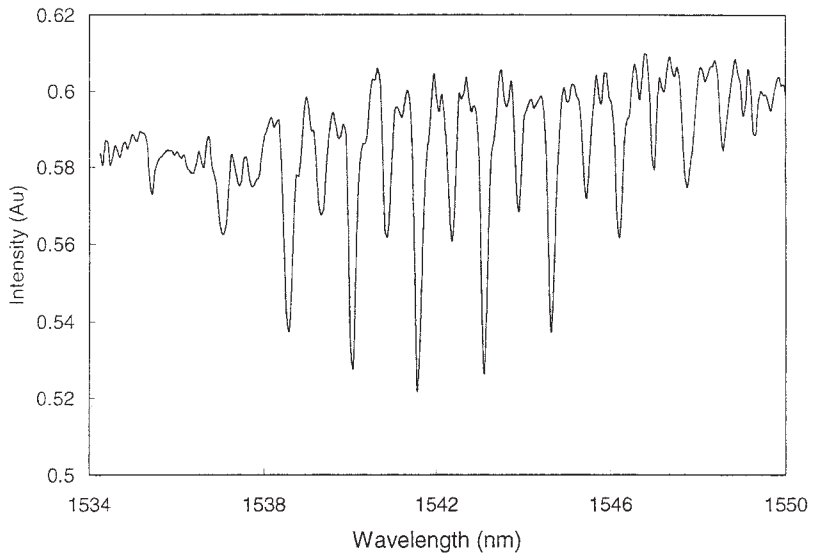

Figure 12 FTIR spectrum of a multimode Bragg grating sensor at room temperature.

gen-cooled environmental chamber. The sensor was cooled from the ambient temperature to −55°C, and its response is shown in Figure 8. The response of the sensor was linear, and the accuracy was ±1°C. The accuracy was limited by the presence of the fan inside the environmental chamber, which caused significant vibrations.

Soda silicate sensor in a microwave oven. The durability and operation of the sensor were further tested in the rugged atmosphere of the microwave oven. When the oven was switched on, the magnetron vibrated periodically, and this caused the response of the sensor to be swamped by noise. The in-house FP sensor was also tested against the commercially available Fiso sensor. The microwave power was raised in increments from 400 to 800 W as the temperature rise was not uniform; the rate of the temperature increase decreased with increasing temperature. Figure 9 shows the response of the sensor to the temperature inside the microwave oven. Data were collected every 20 s. The maximum temperature reached by the sensor was

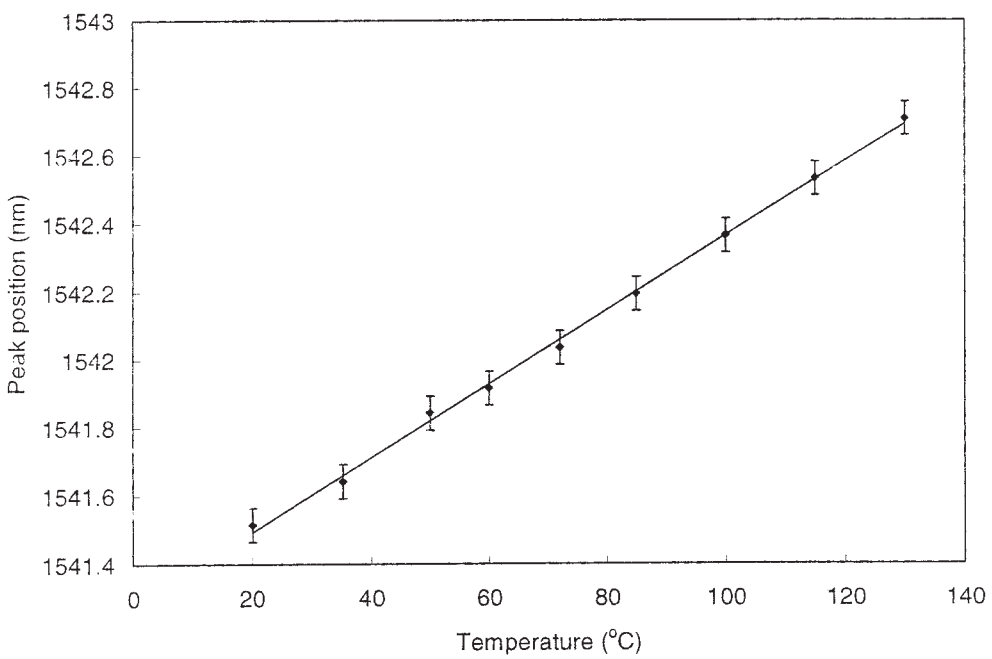

Figure 13 Response of one of the peaks of a multimode Bragg grating sensor to the temperature.

TABLE IV
Range and Accuracy of the Four Optical-Fiber Sensors Described and Tested

Sensor type	Temperature working range (°C)	Accuracy (°C)	Cost
EFPI sensor with a borosilicate capillary	20 to 400	±0.8	£30[a]
EFPI sensor with a sodasilicate reflector	−50 to 20	±1	£30[a]
	20 to 250	±0.5	
Single-mode Bragg grating (849 nm)	20 to 160	±2	£60
Multimode Bragg grating (1540 nm)	20 to 130	±0.5	£60[a]
Commercial sensor from Fiso Technology	FOT-L: −40 to 250	±1	£250
	FOT-H: −40 to 350	±0.5	£350

The commercial sensor is shown for reference.
[a] Estimated cost.

122°C, and the accuracy was calculated to be ±1°C. The output from this sensor was repeatable and linear. This shows that the sensor could readily be used inside the microwave oven for temperature monitoring.

Single-mode bragg grating sensor

A typical reflection spectrum from the single-mode fiber Bragg grating at the ambient temperature is illustrated in Figure 10. This sensor was subjected to a stepwise temperature increment of 10°C from the ambient temperature to 180°C. The spectra from the CCD spectrometer were collected during the hold period. The position of the peak was recorded at each temperature hold and is presented in Figure 11, which shows a linear response. The response to the temperature for this sensor operating at 850 nm was a shift of 5.6 pm $°C^{-1}$. The values quoted in the literature for single-mode fibers range from 5.5 to 6.8 pm $°C^{-1}$.

Multimode bragg grating sensor

Figure 12 shows a typical transmission spectrum from a multimode Bragg grating sensor obtained via the FTIR spectrometer. Sixteen transmission dips were visible, and each was monitored for the temperature-affected peak shift. The response of one of the center peaks (6487 cm^{-1} or 1541 nm) is shown in Figure 13. A linear response was noted during the full temperature range. The shift in the peak was 10.8 pm $°C^{-1}$. The temperature sensitivity of multimode fiber Bragg gratings operating at 1550 and 750 nm has been reported to be 11.5 and 3 pm $°C^{-1}$, respectively.

One limitation of the way in which this sensor was interrogated was that the shift in λ_B as a function of the temperature had to be recorded manually. However, the response time of the sensor could be improved with a fast-scan system and with an algorithm used to convert the peak position directly into the temperature. The accuracy of the sensor with the FTIR spectrometer as the detector was ±0.5°C. This was comparable to the accuracy of the soda silicate reflector sensor with the CCD spectrometer.

Comparison between the sensors

Table IV summarizes all the different sensors investigated in this study, including the commercial sensor purchased from Fiso Technology. Of the four sensors tested, the one made with the soda silicate reflector offers the greatest promise. This sensor has an accuracy comparable to that of the multimode fiber Bragg grating but at half the cost. Furthermore, the interrogation unit is cheaper, and the conversion of the cavity length data to the temperature is simpler.

A comparison between the in-house soda silicate reflector sensor and the commercial FOT-L temperature sensor is given in Table V. There is little difference between the performances of the two sensors. However, the in-house sensor is economically more viable, and this allows it to be used as a disposable sensor during cure monitoring inside a microwave oven. In addition, the sensor has a much smaller diameter, and this allows embedment in the sample more readily than the commercial sensor.

In addition to the differences summarized in Table V between the in-house and commercial sensors, the other difference between these two sensors lies in their con-

TABLE V
Comparison Between the In-House Soda Silicate EFPI Sensor and the Commercially Available FOT-L Temperature Sensor from Fiso Technology

Sensor type	Fiso Technology FOT-L sensor	in-house Soda silicate EFPI sensor
Temperature range	−40 to 250°C	−50 to 250°C
Accuracy	±1°C	±1°C
Probe dimension	1.25-mm o.d.	0.3-mm o.d.
Sensing length	10-mm sensitive zone	8–20 mm (depending on the required sensitivity)

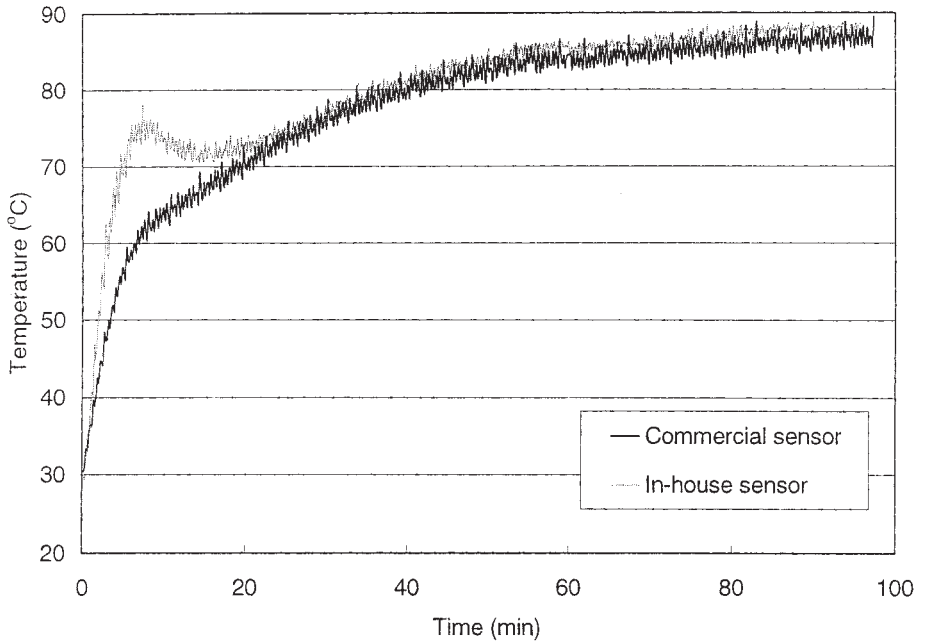

Figure 14 Use of FP (in-house) and Fiso (commercial) sensors for temperature monitoring during curing in a microwave oven.

struction. The commercial sensor used two mirrors that were not attached to the lead-in optical fibers. Furthermore, the commercial sensor used two mirrors deposited on the tip of multimode optical fibers as the FP etalon.[22] In the in-house sensor design, the light guide itself acted as one of the reflectors, and the second reflector was made of a material of a different thermal expansion coefficient to mismatch the expansion.

Further viability test of the soda silicate sensor

Monitoring the cure temperature in a microwave oven

Figure 14 shows the response of the commercial (Fiso Technology) and in-house sensors used to monitor the temperature when the resin was undergoing cure in the microwave oven at a power level of 400 W. An excellent correlation was obtained between the two sensors. However, the output from the in-house FP sensor showed an exotherm, as expected, as the sample started to crosslink. This exotherm was not noticed with the commercial sensor, as the latter could not be placed directly in the sample. This further illustrates the need for a low-cost disposable sensor for monitoring the exact temperature of a resin while it is being processed.

Monitoring the temperature inside a composite

Finally, the sensor was placed between the fourth ply and fifth ply of an eight-ply E-glass fiber/epoxy lam-

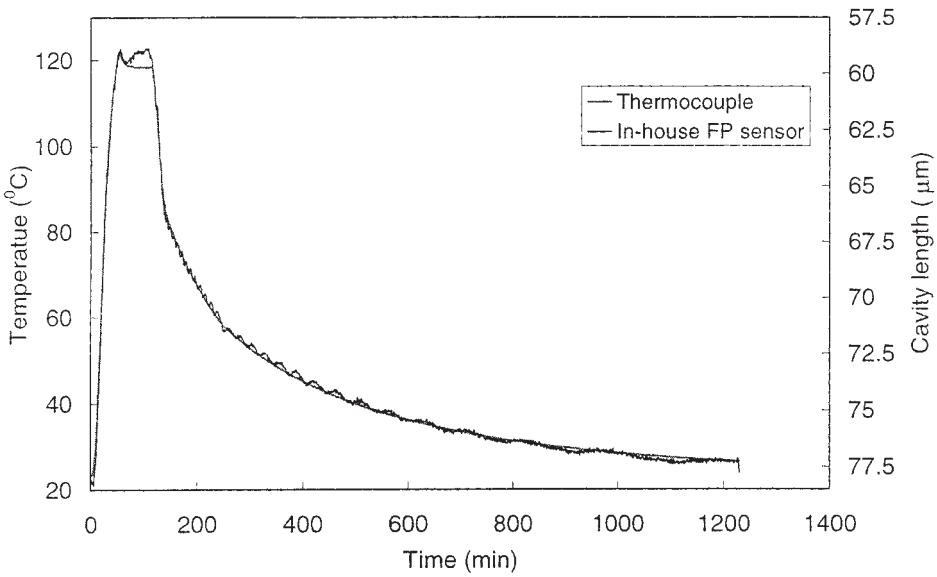

Figure 15 Response of a sensor in an autoclave placed between the fourth ply and fifth ply of a composite laminate.

inate that was cured in an autoclave. The response of the sensor and the actual temperature noted by the thermocouple with the cure time inside the autoclave are shown in Figure 15. The change in the cavity length of the sensor followed the temperature of the autoclave closely. This shows that the sensor could also be embedded in a composite panel and provide the inherent temperature in the middle of a thick laminate.

CONCLUSIONS

In this study, four fiber-optic-based sensor designs were evaluated for temperature-sensing applications. The conventional EFPI sensor design was modified through the mismatching of the coefficients of thermal expansion of either the precision-bore capillary or the reflector fiber. The sensors were evaluated for temperature metrology up to 400 or 320°C. The deployment of an EFPI sensor with a soda silicate reflector from the ambient temperature to −50°C was also conducted successfully. The temperature of a resin system while it was being cured in a microwave oven was monitored with this modified EFPI sensor. The sensor was also used to monitor the temperature of a composite laminate while it was being processed in an autoclave. These results show that this low-cost sensor can be readily used to monitor the temperature in a harsh environment.

The assistance of B. Ralph, M. Keats, R. Badcock, and R. Hall is duly acknowledged. The multimode Bragg sensors used in this study were prepared and supplied by T. Liu.

References

1. Degamber, B.; Fernando, G. F. Mater Res Soc Bull 2002, 27, 370.
2. Measures, R. M. Structural Monitoring with Fibre Optic Technology; Academic: New York, 2001.
3. Trade literature; 2003.
4. Rogers, D. J.; Bialkowski, M. E.; Hill, D. J. T.; George, G. A. High Perform Polym 1998, 10, 341.
5. Hedreul, C.; Galy, J.; Dupuy, J.; Delmotte, M.; More, C. J Appl Polym Sci 1998, 68, 543.
6. Rogers, D. J.; Marand, E.; Hill, D. J. T.; George, G. A. High Perform Polym 1999, 11, 27.
7. Mijovic, J.; Fishbain, A.; Wijaya, J. Macromolecules 1992, 25, 986.
8. Fu, B.; Hawley, M. C. Polym Eng Sci 2000, 40, 2133.
9. Lewis, D. A.; Hedrick, J. C.; Lyle, G. D.; Ward, T. C.; McGrath, J. E. Mater Res Soc Symp Proc 1988, 124, 181.
10. Mullins, J.; Bows, J. Food Additives Contam 1993, 10, 663.
11. Liu, T.; Martin, A.; Badcock, R.; Ralph, B.; Fernando, G. F. Smart Mater Struct 1997, 6, 464.
12. Rao, Y. J. Meas Sci Technol 1997, 8, 355.
13. Udd, E. Fibre Optic Smart Structures; Wiley: New York, 1995.
14. Othonos, A.; Kalli, K. Fibre Bragg Gratings; Artech: Boston, 1999.
15. Othonos, A. Rev Sci Instrum 1997, 68, 4309.
16. Haran, F. M.; Rew, J. K.; Foote, P. D. Meas Sci Technol 1998, 9, 1163.
17. Wanser, K. H. U.S. Pat. 0,584,820,4 (1998).
18. Djambova, T. V.; Mizunami, T. Jpn J Appl Phys 2000, 39, 1566.
19. Zhao, V.; Claus, R. O. Smart Mater Struct 2000, 9, 212.
20. Day, R. J.; Samoladas, E. Sci Eng Compos Mater 1998, 7, 23.
21. Degamber, B.; Fernando, G. F. J Appl Polym Sci 2003, 89, 3868.
22. Choquet, P.; Juneau, F.; Dadoun, F. In Proceedings of the 1999 International Conference of Dam Safety and Monitoring; Three Gorge Project Site: Yichang, China; p 1.